



Short communication

## Nanosized $\text{LiMn}_2\text{O}_4$ powders prepared by flame spray pyrolysis from aqueous solution

Jang Heui Yi<sup>a</sup>, Jung Hyun Kim<sup>a</sup>, Hye Young Koo<sup>a</sup>, You Na Ko<sup>a</sup>,  
Yun Chan Kang<sup>a,\*</sup>, Jong-Heun Lee<sup>b</sup>

<sup>a</sup> Department of Chemical Engineering, Konkuk University, 1 Hwayang-dong, Gwangjin-gu, Seoul 143-701, Republic of Korea

<sup>b</sup> Department of Materials Science and Engineering, Korea University, Anam-dong, Sungbuk-ku, Seoul 136-713, Republic of Korea

### ARTICLE INFO

#### Article history:

Received 24 August 2010

Received in revised form 20 October 2010

Accepted 8 November 2010

Available online 12 November 2010

#### Keywords:

Cathode material

Flame spray pyrolysis

Lithium manganate

### ABSTRACT

$\text{LiMn}_2\text{O}_4$  powders have been directly prepared by flame spray pyrolysis from an aqueous spray solution of the metal salts. The powders prepared at a low fuel gas flow rate ( $3 \text{ L min}^{-1}$ ) comprise particles with a bimodal size distribution, i.e., submicron- and nanometer-sized particles, and have crystal structures of  $\text{LiMn}_2\text{O}_4$  and  $\text{Mn}_3\text{O}_4$  phases. However, the powders prepared at a high fuel gas flow rate ( $5 \text{ L min}^{-1}$ ) comprise nanometer-sized particles and have pure crystal structure of  $\text{LiMn}_2\text{O}_4$  phase. The powders comprising nanosized particles are well crystallized, and the particles have a polyhedral structure. The mean particle size of these powders is 27 nm. The powders prepared directly by flame spray pyrolysis comprise nanosized particles and have the pure crystal structure of  $\text{LiMn}_2\text{O}_4$ , irrespective of the amount of excess lithium in the precursor solution. The initial discharge capacities of these powders increase from 91 to  $112 \text{ mAh g}^{-1}$  when the amount of excess lithium is increased from 0% to 30% of the stoichiometric amount. The optimum amount of excess lithium required to prepare  $\text{LiMn}_2\text{O}_4$  powders with nanosized particles and the maximum possible initial discharge capacity is 10%.

© 2010 Elsevier B.V. All rights reserved.

### 1. Introduction

Currently, extensive studies are being carried on the feasibility of using  $\text{LiMn}_2\text{O}_4$  as a substitute for  $\text{LiCoO}_2$ . This is because  $\text{LiMn}_2\text{O}_4$  is more advantageous than  $\text{LiCoO}_2$  in terms of cost-effectiveness and environment friendliness [1–5]. It is well known that the electrochemical performance of a cathode material is strongly affected by the particle properties such as morphology, specific surface area, crystallinity, and composition [6–9]. In recent years, attempts have been made to use fine cathode powders (powders comprising fine-sized particles) for the development of high-capacity lithium secondary batteries [10–15]. The use of cathode powders comprising nanosized particles has also been investigated because these powders have high charge/discharge rates. The high charge/discharge rates are in turn due to the large electrode/electrolyte interface area achieved when using these powders [16–21].

Various types of cathode powders comprising nanosized particles have been prepared by liquid-solution methods such as the sol-gel method and coprecipitation [22–25]. Liquid-solution methods have the advantage of low preparation temperature. However,

hard aggregation between the nanometer-sized powders occurs during the post-treatment process. Flame spray pyrolysis has been extensively used to prepare cathode and anode powders comprising nanosized particles [21,26–29]. Cathode powders comprising nanosized particles were prepared directly by the flame spray pyrolysis process because of the high temperature of the flame. Therefore, the cathode powders prepared by flame spray pyrolysis had non-aggregation characteristics.  $\text{LiCoO}_2$ ,  $\text{LiV}_3\text{O}_8$ ,  $\text{Li}_4\text{Ti}_5\text{O}_{12}$ ,  $\text{LiFe}_5\text{O}_8$ , and  $\text{LiMn}_2\text{O}_4$  powders prepared by flame spray pyrolysis have been reported to have good electrochemical properties. Flame spray pyrolysis is known to be an efficient continuous process for the large-scale production of cathode powders comprising nanosized particles. However, this method involves the use of non-aqueous solvents such as 2-ethylhexanoic acid, toluene, xylene, and methyl alcohol. For the large-scale production of the above-mentioned type of cathode powders, it is necessary to use aqueous spray solutions prepared from inexpensive metal salt precursors. In previous studies, a gas-assist nozzle was employed to generate fine droplets.

In this study, we prepared  $\text{LiMn}_2\text{O}_4$  cathode powders comprising nanosized particles by flame spray pyrolysis using an aqueous spray solution prepared from inexpensive metal salts. An ultrasonic spray generator was used to generate fine-sized droplets. The electrochemical properties of the prepared  $\text{LiMn}_2\text{O}_4$  cathode powders were investigated.

\* Corresponding author. Tel.: +82 2 2049 6010; fax: +82 2 458 3504.

E-mail address: [yckang@konkuk.ac.kr](mailto:yckang@konkuk.ac.kr) (Y.C. Kang).

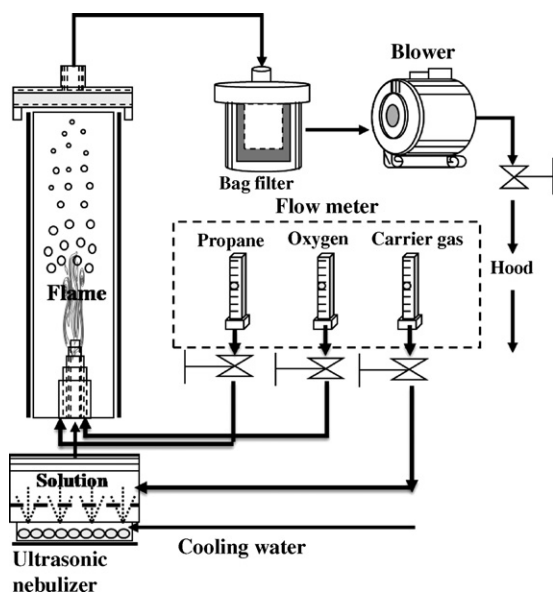


Fig. 1. Schematic diagram of the flame spray pyrolysis process.

## 2. Experimental

As shown in Fig. 1, the flame spray pyrolysis system has a droplet generator, a flame nozzle, a quartz reactor, a powder collector, and a blower. A 1.7-MHz ultrasonic spray generator with six resonators is used to generate droplets, which are then carried into the high-temperature diffusion flame by oxygen (carrier gas). Droplets or powders evaporate, decompose, and melt inside the diffusion flame. Propane (fuel) and oxygen (oxidizer) are used to produce the diffusion flame. The flame nozzle consists of five concentric pipes. Droplets generated from the precursor solution are supplied to the diffusion flame through the central pipe by the carrier gas, whose flow rate is varied appropriately. The flow rate of the fuel gas is changed from 2 to 5 L min<sup>-1</sup>. The flow rates of the oxidizer and carrier gases are fixed at 40 L min<sup>-1</sup> and 10 L min<sup>-1</sup>, respectively. The total concentration of lithium carbonate (LiCO<sub>3</sub>, Aldrich) and manganese acetate hexahydrate (Mn(CH<sub>3</sub>CO<sub>2</sub>)<sub>4</sub>·4H<sub>2</sub>O, Aldrich) is 0.3 M. The amount of excess lithium in the solution is changed from 0% to 30% of the stoichiometric amount.

The charge/discharge capacities of the prepared LiMn<sub>2</sub>O<sub>4</sub> cathode powders were determined. The electrode was fabricated using a mixture of 12 mg of LiMn<sub>2</sub>O<sub>4</sub> and 4 mg of TAB (TAB is a mixture of 3.2 mg of teflonized acetylene black and 0.8 mg of a binder). Lithium metal and a microporous polypropylene film were used as the counter electrode and separator, respectively. The electrolyte (TECHNO Semichem, Co.) was 1 M LiPF<sub>6</sub> in a 1:1 (v/v) mixture of EC/DMC. The entire cell was assembled in a glove box in an argon atmosphere. The charge/discharge characteristics of the samples were determined by potential cycling in the range 3.0–4.3 V at a current density of 0.1 C.

## 3. Results and discussion

The morphologies of the LiMn<sub>2</sub>O<sub>4</sub> powders prepared by flame spray pyrolysis were affected by the type of solvent used and the flow rates of the fuel, oxidizer, and carrier gases. An increase in the flow rate of the fuel gas causes an increase in the temperature and length of the diffusion flame. The flow rate of the oxidizer gas should be optimized to obtain the diffusion flame with high temperature by complete combustion of the fuel gas. The flow rate of the carrier gas will change the residence time of the powders inside the diffusion flame. In this study, we found that complete

evaporation of the Li and Mn components should occur inside the diffusion flame so that nanometer-sized LiMn<sub>2</sub>O<sub>4</sub> powders are obtained. Therefore, the flow rates of the fuel, oxidizer, and carrier gases were optimized in our flame spray pyrolysis process as 5 L min<sup>-1</sup>, 40 L min<sup>-1</sup>, and 10 L min<sup>-1</sup>, respectively. Fig. 2 shows the scanning electron microscopy (SEM) image of the LiMn<sub>2</sub>O<sub>4</sub> powders prepared by flame spray pyrolysis under the optimum preparation conditions, for different amounts of excess lithium in the spray solution. The flow rate of the fuel gas was 5 L min<sup>-1</sup>. All the powders prepared by flame spray pyrolysis comprised nanometer-sized particles and were slightly aggregated, irrespective of the amount of excess lithium. Complete evaporation of the lithium and manganese components occurred inside the high-temperature diffusion flame. Therefore, LiMn<sub>2</sub>O<sub>4</sub> powders comprising nanosized particles were formed by nucleation and growth from the evaporated vapors. Fig. 3 shows the transmission electron microscopy (TEM) images and electron diffraction pattern obtained for the LiMn<sub>2</sub>O<sub>4</sub> powders prepared using the spray solution in which the amount of excess lithium was 10% of the stoichiometric amount. The powder particles were well crystallized and had a polyhedral structure. From the TEM images, the mean size of the powders was determined to be 27 nm. Fig. 4 shows the X-ray diffraction (XRD) patterns of the LiMn<sub>2</sub>O<sub>4</sub> powders prepared using spray solutions with different amounts of excess lithium. The powders prepared directly by flame spray pyrolysis comprised pure LiMn<sub>2</sub>O<sub>4</sub> crystals, irrespective of the amount of excess lithium in the spray solution. The mean crystallite sizes of the LiMn<sub>2</sub>O<sub>4</sub> powders prepared from the spray solutions in which the amount of excess lithium was 0%, 10%, and 30% were 24, 20, and 21 nm, respectively.

The effect of the amount of excess lithium dissolved in the spray solutions on the initial charge/discharge capacities of the LiMn<sub>2</sub>O<sub>4</sub> powders is shown in Fig. 5. The initial discharge capacity changed from 91 to 112 mAh g<sup>-1</sup> when the amount of excess lithium was increased from 0% to 30% of the stoichiometric amount. The optimum amount of excess lithium required for the preparation of LiMn<sub>2</sub>O<sub>4</sub> powders with the maximum initial charge/discharge capacity was 10%.

The effects of fuel gas flow rate on the morphologies and crystal structures of the powders prepared by flame spray pyrolysis are shown in Figs. 6 and 7, respectively. The amount of excess lithium was fixed at 10% of the stoichiometric amount. The powders prepared at a low fuel gas flow rate of 2 L min<sup>-1</sup> comprised submicron-sized hollow spherical particles. In this case, evaporation of the lithium and manganese components did not occur because of the low flame temperature and short flame length. The powders prepared at a fuel gas flow rate of 3 L min<sup>-1</sup> comprised particles with a bimodal size distribution, i.e., the powders comprised both nanometer- and submicron-sized particles. Powders with nanometer-sized particles were formed from the evaporated vapors. Incomplete evaporation of the lithium and manganese components resulted in the formation of powders comprising spherical submicron-sized particles. Complete evaporation of the lithium and manganese components occurred when the fuel gas flow rate was 4 L min<sup>-1</sup>. Therefore, powders comprising nanosized particles with a narrow size distribution could be obtained when the fuel gas flow rate was 4 L min<sup>-1</sup>. The powders prepared at low fuel gas flow rates (<3 L min<sup>-1</sup>) had crystal structure of LiMn<sub>2</sub>O<sub>4</sub> and Mn<sub>3</sub>O<sub>4</sub> phases. At high flame temperatures, the lithium and manganese components had different evaporation characteristics. Therefore, the powders comprising nanosized and submicron-sized particles, prepared at low fuel gas flow rates of less than 3 L min<sup>-1</sup>, had different compositions. On the basis of these observations, we state that it is necessary to ensure complete evaporation of the lithium and manganese components in the spray solution so that phase-pure LiMn<sub>2</sub>O<sub>4</sub> powders comprising nanosized particles are obtained.

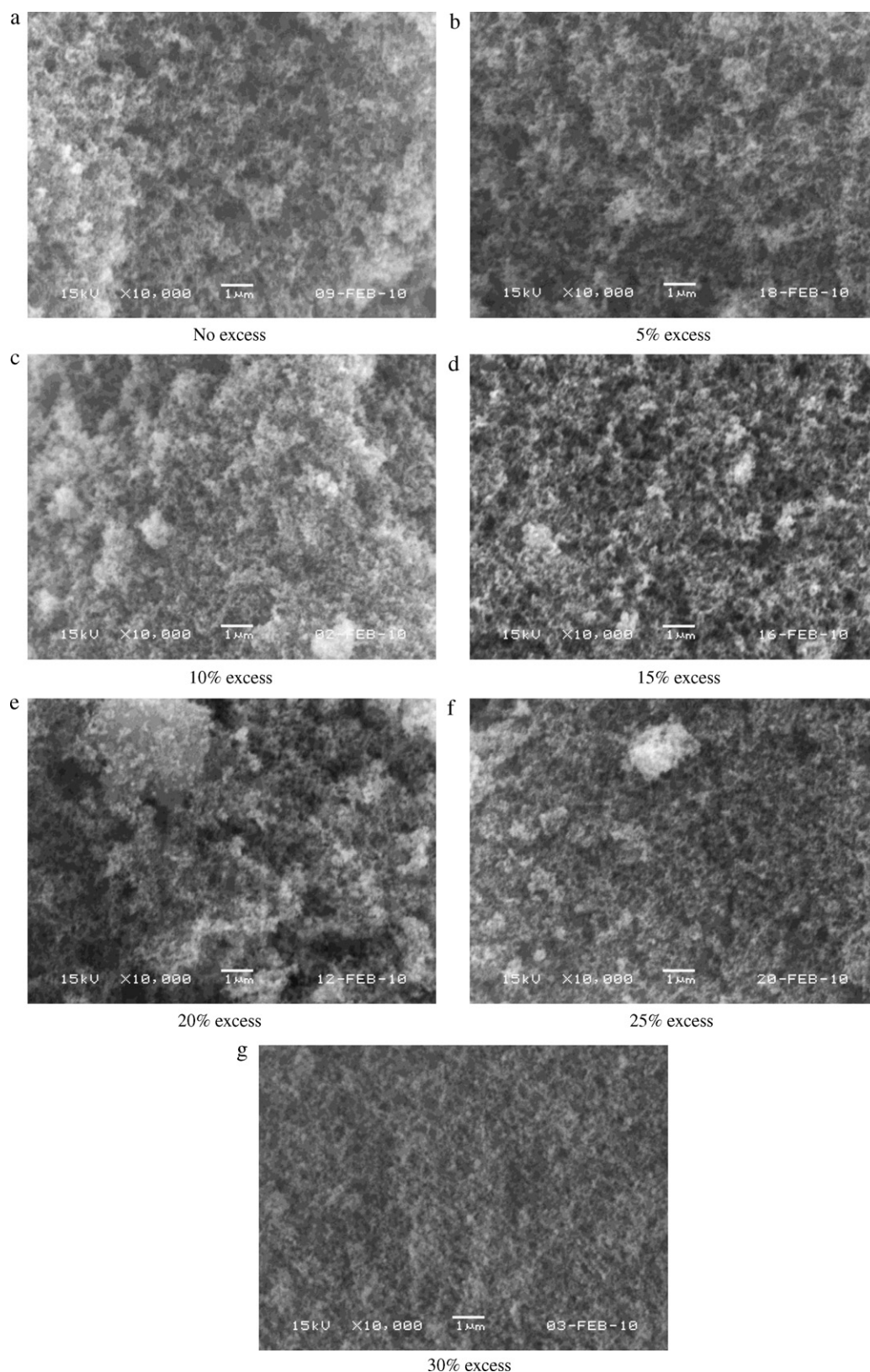
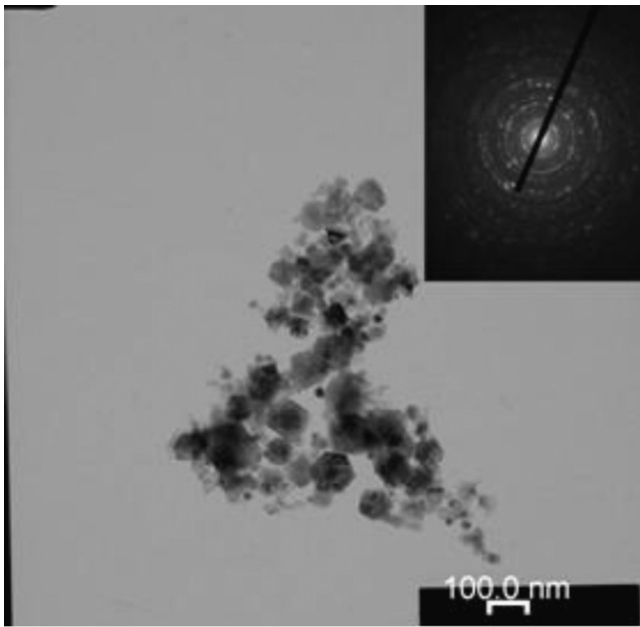


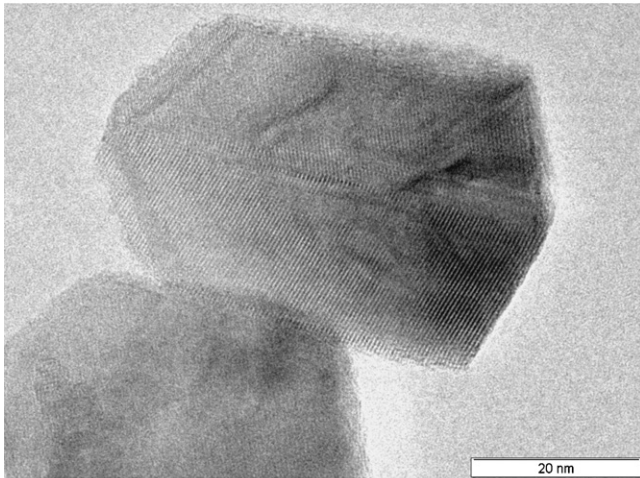
Fig. 2. SEM images of the  $\text{LiMn}_2\text{O}_4$  powders prepared from the spray solutions with different excess amounts of lithium component.

Fig. 8 shows the initial charge/discharge curves for the powders prepared by flame spray pyrolysis at different fuel gas flow rates. The powders prepared at low fuel gas flow rates had low charge/discharge capacities because of the impurity phase present. However, the nanosized-particle-containing  $\text{LiMn}_2\text{O}_4$  powders

prepared at high fuel gas flow rates had high discharge capacity even without post-treatment. The initial discharge capacities of the powders were 54, 53, 102, and 112  $\text{mAh g}^{-1}$  when the fuel gas flow rates were 2, 3, 4, and 5  $\text{L min}^{-1}$ , respectively. Fig. 9 shows the cycle properties of the powders prepared by flame spray pyrolysis for dif-



a low resolution image and electron diffraction



b high resolution image

**Fig. 3.** TEM images of the  $\text{LiMn}_2\text{O}_4$  powders prepared from the spray solution with 10% excess of lithium component.

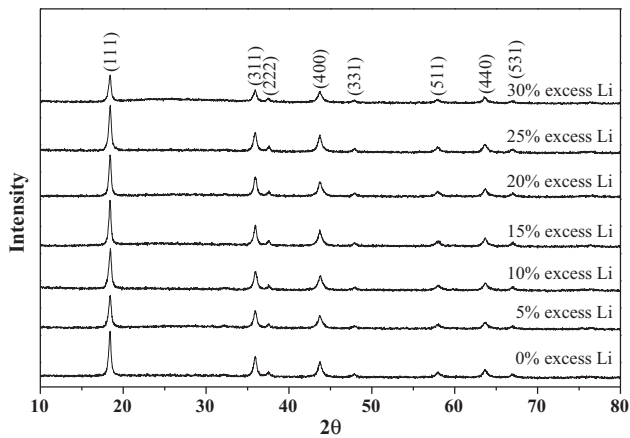


**Fig. 4.** XRD patterns of the  $\text{LiMn}_2\text{O}_4$  powders prepared from the spray solutions with different excess amounts of lithium component.

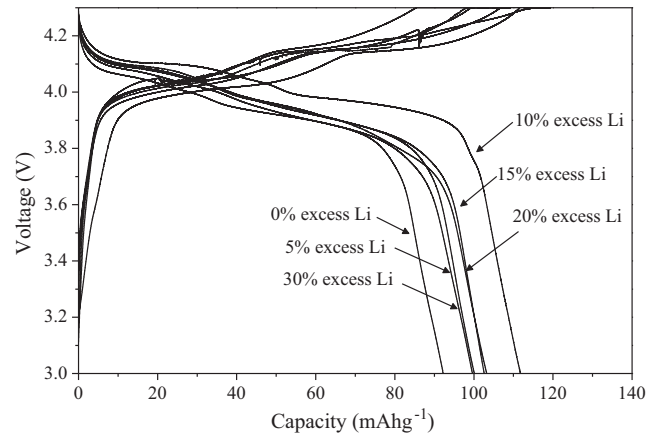
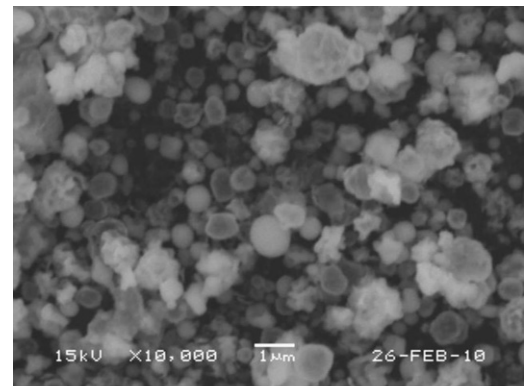
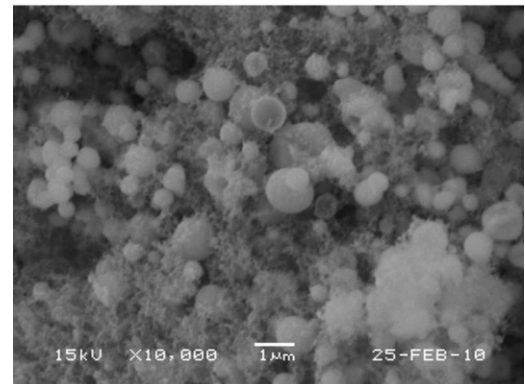


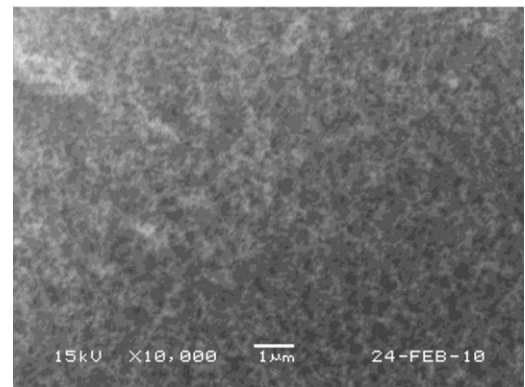
**Fig. 5.** Initial charge/discharge curves of the  $\text{LiMn}_2\text{O}_4$  powders prepared from the spray solutions with different excess amounts of lithium component.



a 2-40-10



b 3-40-10



c 4-40-10

**Fig. 6.** SEM images of the  $\text{LiMn}_2\text{O}_4$  powders prepared at different flow rates of fuel gas (fuel-oxidizer-carrier).

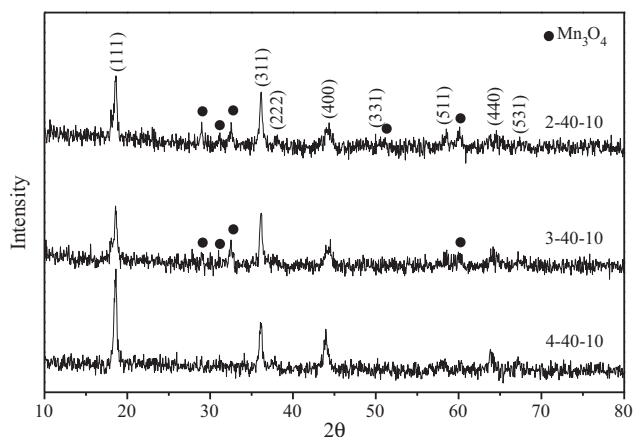


Fig. 7. XRD patterns of the  $\text{LiMn}_2\text{O}_4$  powders prepared at different flow rates of fuel gas.

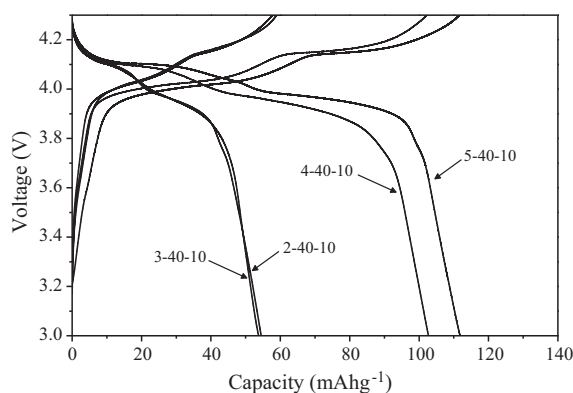


Fig. 8. Initial charge/discharge curves of the  $\text{LiMn}_2\text{O}_4$  powders prepared at different flow rates of fuel gas.

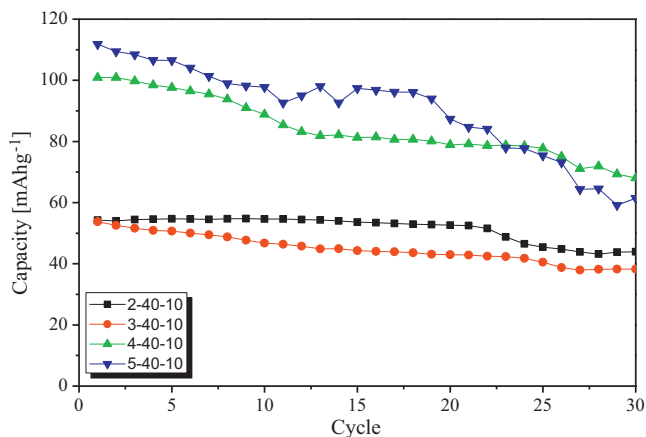


Fig. 9. Cycle properties of the  $\text{LiMn}_2\text{O}_4$  powders prepared at different flow rates of fuel gas.

ferent fuel gas flow rates. The discharge capacities of the powders prepared at a high fuel gas flow rate ( $5 \text{ L min}^{-1}$ ) decreased from  $112 \text{ mAh g}^{-1}$  to  $62 \text{ mAh g}^{-1}$  by the 30th cycle.

#### 4. Conclusions

Lithium and manganese components were found to have different evaporation characteristics in a high-temperature diffusion

flame. Therefore, powders comprising particles with a bimodal size distribution (powders comprising submicron- and nanometer-sized particles) were obtained at low fuel gas flow rates; the charge/discharge capacities of these powders were low because of the presence of impurity phases in the component particles. Complete evaporation of the lithium and manganese components occurred in the high-temperature diffusion flame when the fuel gas flow rate was as high as  $5 \text{ L min}^{-1}$ . The powders prepared directly by flame spray pyrolysis comprised pure  $\text{LiMn}_2\text{O}_4$  crystals when the amount of excess lithium in the precursor solution was increased from 0% to 30% of the stoichiometric amount. The initial charge/discharge capacities of the  $\text{LiMn}_2\text{O}_4$  powders were affected by the amount of excess lithium. The optimum amount of excess lithium required to prepare  $\text{LiMn}_2\text{O}_4$  powders with nanosized particles and the maximum possible initial charge/discharge capacity was 10%.

#### Acknowledgement

This study was supported by a grant (M2009010025) from the Fundamental R&D Program for Core Technology of Materials funded by the Ministry of Knowledge Economy (MKE), Republic of Korea. This study was supported by Seoul R & BD Program (WR090671).

#### References

- [1] Y. Xia, Y. Zhou, M. Yoshio, J. Electrochem. Soc. 144 (1997) 115.
- [2] J.M. Tarascon, D. Guyomard, Electrochim. Acta 38 (1993) 1221.
- [3] T. Ohzuku, M. Kitagawa, T. Hirai, J. Electrochem. Soc. 137 (1990) 769.
- [4] J.M. Tarascon, M. Armand, Nature 414 (2001) 359.
- [5] D. Guyomard, J.M. Tarascon, J. Electrochem. Soc. 138 (1991) 2864.
- [6] T. Ogihara, Y. Yanagawa, N. Ogata, K. Yoshida, Y. Mizuno, S. Yonezawa, M. Takashima, N. Nagata, K. Ogawa, Denki Kagaku Oyobi Kogyo Butsuri Kagaku 61 (1993) 1339.
- [7] T. Ogihara, Y. Saito, T. Yanagawa, N. Ogata, K. Yoshida, M. Takashima, S. Yonezawa, Y. Mizuno, N. Nagata, K. Ogawa, J. Ceram. Soc. Jpn. 101 (1993) 1159.
- [8] Y. Li, C. Wan, Y. Wu, C. Jiang, Y. Zhu, J. Power Sources 85 (2000) 294.
- [9] C.H. Chen, A.A.J. Buysman, E.M. Kelder, J. Schoonman, Solid State Ionics 80 (1995) 1.
- [10] T. Kawamura, M. Makidera, S. Okada, K. Koga, N. Miura, J. Yamaki, J. Power Sources 146 (2005) 27.
- [11] Y. Gu, D. Chen, X. Jiao, J. Phys. Chem. B 109 (2005) 17901.
- [12] O.A. Shlyakhtin, S.H. Choi, Y.S. Yoon, Y.J. Oh, Electrochim. Acta 50 (2004) 511.
- [13] T. Tsuji, T. Kakita, T. Hamagami, T. Kawamura, J. Yamaki, M. Tsuji, Chem. Lett. 33 (2004) 1136.
- [14] S.H. Choi, J.S. Kim, Y.S. Yoon, J. Power Sources 135 (2004) 286.
- [15] J. Liu, Z. Wen, Z. Gu, M. Wu, Z. Lin, J. Electrochem. Soc. 149 (2002) A1405.
- [16] A.S. Arico, P. Bruce, B. Scrosati, J.M. Tarascon, W. van Schalkwijk, Nat. Mater. 4 (2005) 366.
- [17] S.H. Park, S.T. Myung, S.W. Oh, C.S. Yoon, Y.K. Sun, Electrochim. Acta 51 (2006) 4089.
- [18] J.Y. Luo, L. Cheng, Y.Y. Xia, Electrochem. Commun. 9 (2007) 1404.
- [19] Z. Bakenov, M. Wakihara, I. Taniguchi, J. Solid State Electrochem. 12 (2008) 57.
- [20] F.O. Ernst, H.K. Kammler, A. Roessler, S.E. Pratsinis, W.J. Stark, J. Ufheil, P. Novák, Mater. Chem. Phys. 101 (2007) 372.
- [21] T.J. Patey, R. Büchel, M. Nakayama, P. Novák, Phys. Chem. Chem. Phys. 11 (2009) 3756.
- [22] S. Passerini, F. Coustier, M. Giorgetti, W.H. Smyrl, Electrochem. Solid State Lett. 2 (1999) 483.
- [23] A.R. Naghash, J.Y. Lee, J. Power Sources 85 (2000) 284.
- [24] B.J. Hwang, R. Santhanam, D.G. Liu, J. Power Sources 97 (2001) 443.
- [25] A. Subramania, N. Angayarkanni, T. Vasudevan, Mater. Chem. Phys. 102 (2007) 19.
- [26] T.J. Patey, R. Buchel, S.H. Ng, F. Krumeich, S.E. Pratsinis, P. Novák, J. Power Sources 189 (2009) 149.
- [27] T. Lee, K. Cho, J. Oh, D. Shin, J. Power Sources 174 (2007) 394.
- [28] H.D. Jang, C.M. Seong, Y.J. Suh, H.C. Kim, C.K. Lee, Aerosol Sci. Technol. 38 (2004) 1027.
- [29] T.J. Patey, S.H. Ng, R. Buechel, N. Tran, F. Krumeich, J. Wang, H.K. Liu, P. Novák, Electrochem. Solid State Lett. 11 (2008) A47.